

# Multi-scale Anomaly Detection for Big Time Series of Industrial Sensors

Quan Ding  
Shenghua Liu  
Bin Zhou  
Huawei Shen  
Xueqi Cheng

DINGQUAN20@MAILS.UCAS.AC.CN  
LIUSHENGHUA@ICT.AC.CN  
ZHOUBIN17G@ICT.AC.CN  
SHENHUAWEI@ICT.AC.CN  
CXQ@ICT.AC.CN

*Institute of Computing Technology, Chinese Academy of Sciences*

## Abstract

Given a multivariate big time series, can we detect anomalies as soon as they occur? Many existing works detect anomalies by learning how much a time series deviates away from what it should be in the reconstruction framework. However, most models have to cut the big time series into small pieces empirically since optimization algorithms cannot afford such a long series. The question is raised: *do such cuts pollute the inherent semantic segments, like incorrect punctuation in sentences?*

Therefore, we propose a reconstruction-based anomaly detection method, MissGAN, iteratively learning to decode and encode naturally smooth time series in coarse segments, and finding out a finer segment from low-dimensional representations based on HMM. As a result, learning from multi-scale segments, MissGAN can reconstruct a meaningful and robust time series, with the help of adversarial regularization and extra conditional states. MissGAN does not need labels or only need labels of normal instances, making it widely applicable. Experiments on industrial datasets of real water network sensors show our MissGAN outperforms the baselines with scalability. Besides, we use a case study on the CMU Motion dataset to demonstrate that our model can well distinguish unexpected gestures from a given conditional motion.

**Keywords:** Big Time Series; Reconstruction; Anomaly Detection; Multi-scale Training; Segmentation; GAN Network; GRU

## 1. Introduction

Big time series are generated from countless domains, such as infrastructure, system monitoring, personal wearable devices, and medical analysis [Faloutsos et al. \(2019\)](#). While big time series always have a long length, detecting the anomalies in such multivariate time series is a key to secure infrastructures and systems functioning, and diagnose the anomalies of people’s motion and health data. However, traditional supervised machine learning methods cannot handle this task properly, because of the inherent nature that labeled anomalies are far fewer, and anomalies arise differently from each other, i.e., obtaining accurate and representative features is challenging [Chandola et al. \(2009\)](#). Thus the question is raised:

*How can we detect anomalies in big time series, when observing only normal time series or observed data being normal most of the time?*

Some existing works [Kiat Lim et al. \(2018\)](#); [Wang et al. \(2019\)](#) augment anomalous instances from labeled anomalies to balance the training. Those methods assume that the existing labeled anomalies are representative, without considering unseen types of anomalies. The non-supervised

methods, either learning only from labeled normal instances or only from unlabeled data (containing very few anomalies) perform promisingly and are widely applicable in anomaly detection [Chalapathy and Chawla \(2019\)](#); [Chandola et al. \(2009\)](#); [Hooi et al. \(2017\)](#). Among those methods, the reconstruction of data is the most frequently used framework, and anomalies produce high reconstruction error [Shah et al. \(2014\)](#). Auto-encoders (AE) [Han et al. \(2011\)](#) allows for more complex patterns by applying nonlinear functions for reconstruction and anomaly detection. Moreover, combined with GAN [Goodfellow et al. \(2014\)](#), the performance of the encoder-decoder model improves further via adversary regularization.

GAN is used widely on reconstruction-based anomaly detection task. AnoGAN [Schlegl et al. \(2017\)](#) is the first application of GAN on medical images whose running consumes a great deal of time. Later work Ganomaly [Akçay et al. \(2018\)](#) and EGBAD [Zenati et al. \(2018\)](#) focus on adding a coding part for an end-to-end model. In terms of time series anomaly detection, GAN-based models [Zhou et al. \(2019\)](#); [Li et al. \(2019\)](#) reconstructed the given time series segments for anomaly detection, for example, real-valued medical time series [Esteban et al. \(2017\)](#). Variant of computing the loss of GAN is applied in BeatGAN [Zhou et al. \(2019\)](#) which performs well on ECG data. MAD-GAN [Li et al. \(2019\)](#) combines LSTM-RNN with the GAN framework and reports good results on the SWaT dataset. However, its inefficiency in calculating the best match for each test case limits its application. Most of these models use the sliding window algorithm to segment big time series which may produce pathologically poor results under some circumstances [Keogh et al. \(2004\)](#). Thus, the second question is raised:

*How can we find out a group of cutting points that follows the inherent characteristics of big time series data?*

Multi-scale segmentation and feature extraction are broadly used in image processing [Tabb and Ahuja \(1997\)](#). [Zeune et al. \(2017\)](#) uses multi-scale segmentation on images to find multiple objects with different scales. Transferring the idea into time series, [Cho and Fryzlewicz \(2012\)](#) tries to locate breakpoints in different scales. AutoPlait [Matsubara et al. \(2014\)](#) and its variant Neucast [Chen et al. \(2018\)](#) use the HMM-based model and MDL principle to make segmentations.

Therefore, we propose MissGAN, simultaneously multi-scale reconstruction and segmentation for big time series anomaly detection (see Fig 1). Our method exploits extra conditional information to reconstruct multi-mode time series, and outputs explainable results by reconstruction error, pinpointing the specific anomalous time ticks. Experiments on time series from SWaT testbed and CMU Motion Capture data show the effectiveness and robustness of our MissGAN.

In summary, our main contributions are summarized as follows:

- **Multi-scale reconstruction:** MissGAN iteratively learns to reconstruct from initially coarse and long segments of time series, and with learned hidden representation, MissGAN finds proper cuts on current segments in turn to optimize reconstruction. In such a way, reconstruction is gradually improved by training on multi-scale segments of big time series, i.e., from coarse to fine-grained. Moreover, with conditional reconstruction, MissGAN can generate multi-mode time series given different states.
- **Effectiveness:** Experiments on the publicly available data show that our method outperforms the baselines, including both linear and non-linear models in anomaly detection. On the motion dataset, MissGAN can be trained to reconstruct well from the given walking and running time series and discriminates against other types of unexpected gestures.

Table 1: Comparison with related methods.

methods	non-linear	explainability	extra conditions	multi-scale segmentation
PCA <a href="#">Li and Wen (2014)</a>		✓		
KNN <a href="#">Angiulli and Pizzuti (2002)</a>	✓	✓		
BeatGAN <a href="#">Zhou et al. (2019)</a>	✓	✓		
LSTM-AE <a href="#">Malhotra et al. (2016)</a>	✓	✓		
MAD-GAN <a href="#">Li et al. (2019)</a>	✓	✓	?	
MissGAN	✓	✓	✓	✓

- **Explainability:** MissGAN can pinpoint the exact time ticks when anomalies occur in a segment of time series, routing people’s attention to diagnosis.
- **Scalability:** Our method can detect anomalies in 1.78 ms/tick on average, linear in the size of the total time series.

MissGAN is open-sourced for reproducibility<sup>1</sup>.

## 2. Related Work

The main purpose of anomaly detection is to identify anomalous cases that deviate far from the distribution learned during the training with normal data. Given the reality that labeled anomaly data lacks, unsupervised algorithms are preferred. Refer to [Li et al. \(2019\)](#), anomaly detection algorithms can be classified into three categories: i) linear model based method, ii) distance and probabilistic based method and iii) deep learning based method.

**Linear methods.** Principal Component Analysis (PCA) [Li and Wen \(2014\)](#) is the most familiar approach to most of us. As a multivariate data analysis method, PCA extracts information and reduce dimensions from highly correlated data by orthogonal transformation.

**Distance and probabilistic based methods.** K-Nearest Neighbor (KNN) is a popular method which calculates the anomaly score by computing average distance to K nearest neighbors [Angiulli and Pizzuti \(2002\)](#). Although this method seems simple and effective, we still need some prior knowledge to improve its performance, such as numbers of anomalies or numbers of clusters. Yeh, *et al.* proposed a parameter-free, fast and general algorithm Matrix Profile [Yeh et al. \(2016\)](#) to solve various time series problems. Another problem of distance based method is how to segment time series properly. Probabilistic based method can be regarded as upgrades of distance based methods with regarding to the data distributions. For example, Feature Bagging (FB) method [Lazarevic and Kumar \(2005\)](#) pays attention to the correlations of variables and performs well. Other works such as Hidden Markov Models [Baum and Petrie \(1966\)](#) is of great use for segmentation. [Molina and Pla \(2001\)](#) proposed methods to detect clause. Variations like DynaMMo [Li et al. \(2009\)](#) and AutoPlait [Matsubara et al. \(2014\)](#) segmented series on vocabulary-learning rules. Recent work like BeatLex [Hooi et al. \(2017\)](#) utilized Minimum Description Length (MDL) to learn vocabularies. These methods have made progress compared to traditional sliding window methods. Yet, distributions of temporal data are volatile and hard to observe and thus these methods are not welcome in some applications.

1. <https://www.dropbox.com/sh/pnn4mjbpltdlzbzf/AADu9Brpym3WrHDwbrfLUEM4a?dl=0>

**Deep Learning based methods** have made great improvements and gains so much popularity ever since the boosting development of big data and deep learning architectures. Autoencoder Han *et al.* (2011) is used widely benefiting from its ability of coding and reconstructing to catch features. LSTM-AE Malhotra *et al.* (2016) detects anomalies by reconstructing and calculating anomalousness score based on LSTM cells. Kieu *et al.* Kieu *et al.* (2019) propose ensemble frameworks based on sparsely-connected RNN to do unsupervised outlier detection. Xu *et al.* propose Donut Xu *et al.* (2018), which is also an autoencoder-based model designed for time series anomaly detection. Recently, the generative adversarial network has shown great ability in learning data features and distributions. Therefore, it has been deployed on image processing tasks, such as generating synthetic images Di Mattia *et al.* (2019). AnoGAN Schlegl *et al.* (2017) is the first application of GAN on medical images whose running consumes a great deal of time. Later work Ganomaly Akcay *et al.* (2018) and EGBAD Zenati *et al.* (2018) focus on adding a coding part for an end-to-end model. Furthermore, more and more works pay attention to the application of GAN on generating time series sequences, for example, real-valued medical time series Esteban *et al.* (2017). Luo *et al.* propose  $E^2$ GAN Luo *et al.* (2019) to do time series imputation. Reconstruction based anomaly detection method is applied in BeatGAN Zhou *et al.* (2019) which performs well on ECG data. MAD-GAN Li *et al.* (2019) combines LSTM-RNN with the GAN framework and reports good results on the SWaT dataset. However, its inefficiency in calculating the best match for each test case limits its application. Besides, Hundman *et al.* propose an unsupervised anomaly detection approach Telemanom Hundman *et al.* (2018) which uses LSTMs to predict highvolume telemetry data. Nevertheless, the aforementioned methods can only run on fixed-length segments and cannot utilize conditional information.

Table 1 summarizes the comparison of the related works with our MissGAN in the four characteristics. We use a non-linear method to handle the more sophisticated dataset. Explainability requires results of methods can direct people’s attention to anomalies. Extra conditions stand for the ability of the model to utilize extra information, i.e., labels. Multi-scale segmentation means whether the model can segment data dynamically. The question mark means that MADGAN concatenates those extra conditions as input time series. We can see that only MissGAN meets all the characteristics.

### 3. Proposed Model

Let  $\mathbf{x} = \{x_0, x_1, \dots\}$  be a multivariate time series, where each point  $x_i \in \mathbf{R}^M$  consists of  $M$  dimensions which read from  $M$  different sources at time  $t_i$ . A segment  $\mathbf{x}_j$  is defined as small fragment data extracted from  $\mathbf{x}$  and denotes as  $\mathbf{x}_{\rho_j}^{\rho_j+l_j} \in \mathbf{R}^{M \times l_j}$  where  $\rho_j$  is the start point and  $l_j$  is the length of the segment. Inside each segment  $\mathbf{x}_j$  exists  $M$  readings that record real-time data. We use  $\mathbf{y}$  to stand for the categorical data that is auxiliary to realize features and distributions.

The existing deep learning method shall always divide input series into fixed-length segments which we believe may cause bad effects in training. As a result, our first mission is to segment input series with a proper length  $l$  to construct a collection of segments  $\mathcal{S}$ . With segments divided properly, we can then finish our second mission which is described as:

**Informal Problem 1 (Anomalous time series detection)** *Given a big time series  $\mathbf{x}$  of  $M$  dimensions from daily monitoring of running systems or personal wearable sensors, and their states  $\mathbf{y}$ , knowing that at most of the time the systems or people are normal under states  $\mathbf{y}$ ,*

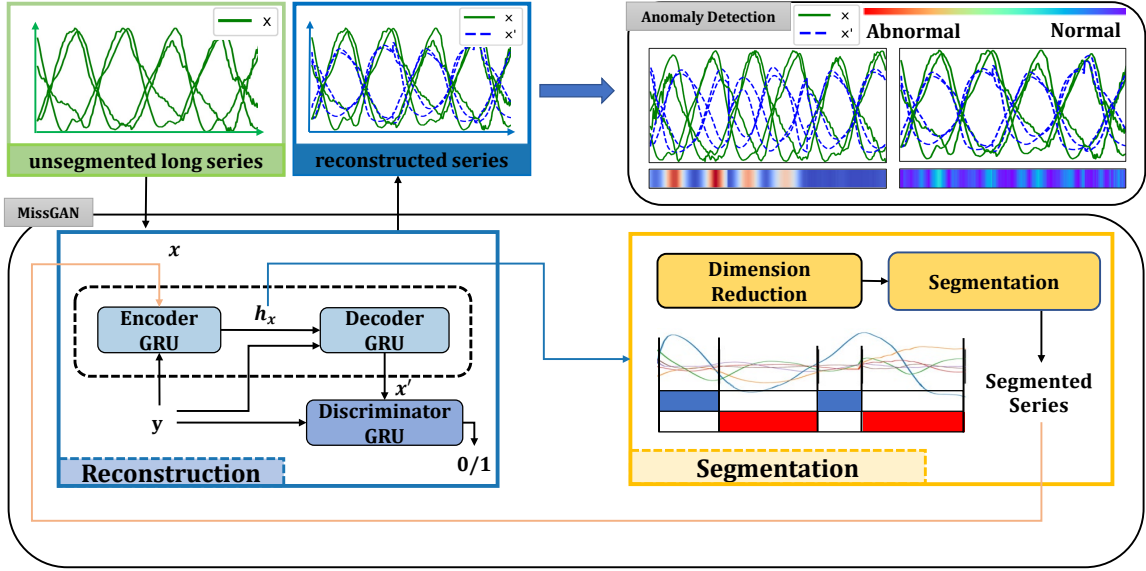


Figure 1: Overview of MissGAN.

- *to detect anomalies happening in time series  $x$ ,*
- *such that the anomalous time ticks of time series deviate far from what they are supposed to be (reconstructed).*

### 3.1. Framework Overview

As Fig 1 shows, our proposed model consists of two parts. The first part is called reconstruction, which is responsible for training a network that combines the discriminator of classic conditional GAN with an extra encoder-decoder network being its reconstruction framework to minimize the reconstruction error as Eq (1) shows. Details of the reconstruction model is introduced in Sec 3.2. Furthermore, to explore an appropriate segmentation for a better reconstruction, we exploit an HMM-based segmenting algorithm which is introduced in Sec 3.3.

$$L = \|x - G_D(G_E(x))\|_2 \quad (1)$$

In testing phase, to judge whether a segment  $x_j$  is anomalous, we reconstruct the segment  $x_j$  using our generator  $G$  and calculate the anomalousness score. Because our model is trained by normal data, we can assert that the segment deviates far from the normal distribution shall get a bad reconstruction, i.e., a relevant high anomalousness score shown in Eq (2), where  $x_{j_t}$  is the data vector of time tick  $t$  and  $x'_{j_t}$  is the reconstructed data vector.

$$A(x_{j_t}) = \|x_{j_t} - x'_{j_t}\|_2, x_{j_t} \in x_j \quad (2)$$

### 3.2. Reconstruction Model

As illustrated in Fig 1, our reconstruction network consists of an encoder-decoder framework and a discriminator of the classic GAN network. Both encoder and decoder are implemented by GRU. Extra information, i.e., conditional dimension  $\mathbf{y}$  is directly added to both the encoder and decoder to take control of the reconstruction of different modes of data. So the total input for each GRU cell is the concatenation of  $x_t$  and  $y_t$ . The encoder  $G_E(\mathbf{x})$  encodes the input  $\mathbf{x}$  to a hidden representation  $\mathbf{h}$  to extract its features. The last hidden state of the encoder is fed into the decoder as its first hidden state. And the decoder  $G_D(\mathbf{x})$  reconstructs the time series  $\mathbf{x}'$  in a reversed order.

The classical conditional GAN framework includes two parts: the generative part  $G$  is responsible for capturing the distribution of input data  $p_x$  and the discriminative part is designed for estimating the probability that the input sample is concocted by the generator rather than extracted from real data  $\mathbf{x}$ . In practice, we don't directly use the classic loss function of the generator due to different frameworks of the generator. Instead, we use pairwise feature matching loss designed for minimizing the distance from the origin data to the generated time series. Regard  $f_D(\cdot)$  as the activation vector located at the hidden layer of the discriminator, we combine the actual distance from origin time series  $\mathbf{x}$  to reconstructed time series  $G_D(G_E(\mathbf{x}))$  with the pairwise feature matching loss accompanied by a regularization parameter  $\lambda$ :

$$L_G = \|\mathbf{x} - G_D(G_E(\mathbf{x}))\|_2 + \lambda \|f_D(\mathbf{x}|\mathbf{y}) - f_D(G_D(G_E(\mathbf{x}))|\mathbf{y})\|_2 \quad (3)$$

Meanwhile, the target of the discriminator  $D$  is to reduce the probability that mistaking reconstructed samples as origin samples. That's to maximize:

$$L_D = \log D(\mathbf{x}|\mathbf{y}) + \log(1 - D(G_D(G_E(\mathbf{x}))|\mathbf{y})) \quad (4)$$

### 3.3. Segmentation Model

We use a two-tier HMM-based method to find a set of cut points  $p = \{\rho_1, \rho_2, \rho_3, \dots\}$  for segmentation, where the *regime* is defined as a group of segments, and each segment has an assignment to one of the several regimes. Let  $\theta$  be HMM model parameters for a regime, including initial state probability, state transition probability, and output probability. Regimes are then modeled by HMM with parameters, i.e.,  $\theta_1, \dots, \theta_r$ , and regime transition matrix denotes as  $\Delta_{r \times r}$ , where  $r$  is the regime size.

Model parameters are learned based on the MDL (minimum description length) principle to minimize the total cost  $Cost(\mathbf{x}, \Theta_H)$  shown in Eq 5. This cost includes three parts:  $Cost_{model}$  describes the coding length of model parameters,  $Cost_{assign}$  calculates the coding length of pattern assignment and the cut points, and  $Cost_{like}$  refers to the likelihood of such assignment by a negative log-likelihood function. Besides, the construction of regimes plays a vital role in the segmentation task, a large granularity may concatenate several patterns into one regime and a small granularity may produce several fractured regimes. So referring to Chen et al. (2018), we adapt the formula of calculating total cost by adding a hyper-parameter  $\alpha$  for controlling the granularity of distinct patterns and assign a default value of 0.1.

$$Cost(\mathbf{x}; \Theta_H) = \alpha \times Cost_{model}(\Theta_H) + Cost_{assign} + Cost_{like}(\mathbf{x}|\Theta_H) \quad (5)$$

In general, we firstly preprocess origin data  $\mathbf{x}$  and divide them coarsely into long series  $\mathbf{x}_{init}$  with length manually assigned, i.e.,  $l_{init}$  and construct the collection of segments  $\mathcal{S}$ . This initial

---

**Algorithm 1** MissGAN Algorithm

---

```
1:  $\Theta_G, \Theta_D, \Theta_H \leftarrow$  initialize parameters
2: Sample segments  $\mathcal{S}(0) = \{\mathbf{x}_1, \dots, \mathbf{x}_m\} \sim$  a batch of long fragments of time series
3: for  $k = 1, 2, \dots, K$  do
4:    $\mathcal{S}(k) = \mathcal{S}(k-1)$  ▷ Segmentation Iterations
5:   for  $i = 1, 2, \dots$  do
6:     Sample  $\{\mathbf{x}_1, \mathbf{x}_2, \dots, \mathbf{x}_j\}$  from  $\mathcal{S}(k)$  ▷ Reconstruction Iterations
7:     Reconstruct  $\{\mathbf{x}'_1, \mathbf{x}'_2, \dots, \mathbf{x}'_j\}$  by  $G_E, G_D$  and  $D$  ▷ Reconstruction
8:     Compute  $L_D$  by Eq (4)
9:      $\Theta_D \leftarrow \Theta_D + \beta \nabla_{\Theta_D}(L_D)$  ▷  $\nabla$  is the gradient
10:    Compute  $L_G$  by Eq (3)
11:     $\Theta_G \leftarrow \Theta_G + \beta \nabla_{\Theta_G}(L_G)$  ▷  $\nabla$  is the gradient
12:  end for
13:   $\mathbf{h}_x =$  hidden representation in  $G_E$ 
14:   $\mathcal{S}(k) =$  fine segments by minimizing Eq (5) ▷ Segmentation
15:  if  $\mathcal{S}(k) \equiv \mathcal{S}(k-1)$  then
16:    break
17:  end if
18: end for
19:  $\mathbf{x}' =$  final training reconstruction model with last  $\mathcal{S}$  as step 6-11
```

---

length is always large enough to contain several periods of data, and we feed these segments  $\mathbf{x}_{init}$  into the reconstruction framework and fetch the latent-space representation  $\mathbf{h}_x$  coded by its encoder part. Then, considering repetitive information may hide in the latent-space representation, we reduce the dimension of hidden representation from  $d_h$  to  $d_r$  by PCA. The HMM-based segmentation model will process the results to search for proper cut points making up of collection  $p$ . Finally, we re-segment origin time series with the known cut points and feed back the newly segmented series collection  $\mathcal{S}'$  into reconstruction part and continue training to get a new updated latent-space representation  $\mathbf{h}_x$ . With adequate iterations, we can extract the cut point data  $p$  from the assigned result. The final collection of segments  $\mathcal{S}$  will then be used to train the reconstruction network.

### 3.4. Proposed MissGAN

MissGAN first trains with coarse-segmented time series and outputs hidden representations as well as learns currently best segmentation. In turn, these optimized segments are fed back to train reconstruction. In such a way, the whole process is optimized until no more segmentation.

Let  $\mathcal{S}(k) = \{\mathbf{x}_1, \mathbf{x}_2, \dots\}$  be segmentation results in the  $k$ -th iteration. Therefore, the overall reconstruction optimizes loss on multi-scale segments of time series, as follows.

$$L_G = \sum_{k=1}^K \sum_{\mathbf{x} \in \mathcal{S}(k)} (\|\mathbf{x} - G_D(G_E(\mathbf{x}))\|_2 + \lambda \|f_D(\mathbf{x}|\mathbf{y}) - f_D(G_D(G_E(\mathbf{x}))|\mathbf{y})\|_2)$$
$$L_D = \frac{1}{K} \sum_{k=1}^K \sum_{\mathbf{x} \in \mathcal{S}(k)} [\log D(\mathbf{x}|\mathbf{y}) + \log(1 - D(G_D(G_E(\mathbf{x}))|\mathbf{y}))]$$

Table 2: General Description of Dataset.

Item	SWaT	Motion
Data Dimensions	25	4
Conditional Dimensions	26	2
Training Size (time ticks)	496,800	8,224
Testing Size (time ticks)	449,919	2,085
Normal Rate <sup>1</sup>	88.02	79.77

<sup>1</sup> Normal Rate is the percentage of normal data in testing data

Finally, A summary of the overall algorithm is depicted in Alg 1.

## 4. Experiment

Experiments are designed to answer the following questions:

**Q1. Accuracy:** How accurately does our method find out anomalies compared with baselines.

**Q2. Effectiveness and explainability:** How effectively does MissGAN find out anomalies in the data of both real-world system sensors and personal wearable motion sensors? How well does MissGAN pinpoint anomalous time ticks of input time series and route people’s attention?

**Q3. Scalability:** How fast does MissGAN test on samples? What is the relation between running time and test sample length?

**Q4. Robustness and parameter sensitivity:** How sensitive does MissGAN react to changes in parameters?

### 4.1. Dataset

We evaluate our proposed method on two datasets. The first one is the secure water treatment system (SWaT) dataset [Mathur and Tippenhauer \(2016\)](#). A total of 25 dimensions that record readings of sensors are regarded as input dimensions while the other 26 dimensions which record states of actuators are regarded as additional information, i.e., the conditional dimensions. The second dataset comes from a motion dataset captured by CMU. This dataset includes motions such as walking, jumping, running, hopping, etc. recorded by 4 sensors, i.e., left and right arms and legs. As there are exact labels for each segment of running and walking, we regard the labels as conditional dimensions. Detailed information of the aforementioned datasets is depicted in Table 2.

### 4.2. Baselines and metrics

The baselines include BeatGAN [Zhou et al. \(2019\)](#), LSTM-AE [Malhotra et al. \(2016\)](#) and MADGAN [Li et al. \(2019\)](#). Parameters of these methods are adjusted well to get their best performances. Besides, we also implement CRGAN, which is MissGAN without multi-scale segmentation, and AEGAN, which is MissGAN without PCA processing to do ablation experiments.

MissGAN calculates the anomalousness score for each time tick in the evaluation dataset. To make a comparison with baselines, we first standardize the anomalousness score by min-max scaling to  $0 \sim 1$ . Then we use two metrics, AUC (Area Under ROC Curve) and ideal F1 score. Given

different thresholds, we get different precision and recall values. The best value will be treated as our ideal F1 score.

Table 3: Performance of each method on AUC score and ideal F1 score based on the results of SWaT dataset, repeated 5 times.

Method	AUC Score	Ideal F1 Score
BeatGAN	$0.8143 \pm 0.0027$	$0.7699 \pm 0.0109$
LSTM-AE	$0.8137 \pm 0.0077$	$0.7780 \pm 0.0037$
MAD-GAN	–	0.77
CRGAN	$0.8217 \pm 0.0120$	$0.7752 \pm 0.0034$
AEGAN	$0.8242 \pm 0.0120$	$0.7830 \pm 0.0120$
MissGAN	<b><math>0.8426 \pm 0.0060</math></b>	<b><math>0.7844 \pm 0.0019</math></b>
MissGAN <sub>0.5%</sub>	$0.8381 \pm 0.0084$	$0.7808 \pm 0.0023$
MissGAN <sub>1.0%</sub>	$0.8348 \pm 0.0089$	$0.7799 \pm 0.0009$

### 4.3. Accuracy and comparison (Q1)

**Experimental setup** We choose GRU [Chung et al. \(2014\)](#) with a single layer of 100 hidden neurons in the encoder, decoder, and discriminator structure. Adam optimizer is used with the learning rate  $\beta$  initialized as 0.001, and decayed by 25% for every 8 epochs. We set the regularization parameter,  $\lambda$  as 0.1 according to results of parameter sensitive experiments. We reduce the dimensions by PCA from  $d_h = 100$  to  $d_r = 6$  before feeding to the segmentation model. Granularity controlling hyper-parameter  $\alpha$  in the segmentation model is set as 0.1 referred to [Chen et al. \(2018\)](#).

**Results.** Table 3 shows the ideal F1 score and AUC score of MissGAN and baselines. Results of MADGAN is extracted from [Li et al. \(2019\)](#). MissGAN outperforms all baseline methods on the ideal F1 score. About the AUC score, MissGAN exceeds other baselines for at most 0.0289.

CRGAN is MissGAN without the segmentation part which is intended to show the effectiveness of segmentation. From Table 3, our proposed MissGAN outperforms CRGAN both on ideal F1 score and AUC score which demonstrates multi-scale segmentation do make contributions to train the model. AEGAN is MissGAN with hidden dimensions in GRU equalling to the reduced dimension after PCA processing in MissGAN which demonstrates the effectiveness of dimension reduction by PCA. We also use this dataset to design experiments on evaluating the robustness of our MissGAN by adding anomalous cases (0.5% and 1.0% of total time tick) to training data.

### 4.4. Effectiveness and explainability (Q2)

We use Mocap dataset to do a case study to demonstrate the effectiveness and explainability. In this experiment, we adjust the granularity controlling hyper-parameter for segmentation model  $\alpha$  as 0.2 to make the best fit for the dataset. In this case, we use running and walking data with different conditional dimensions to train our model, while the remained hopping and jumping data are regarded as abnormal cases.

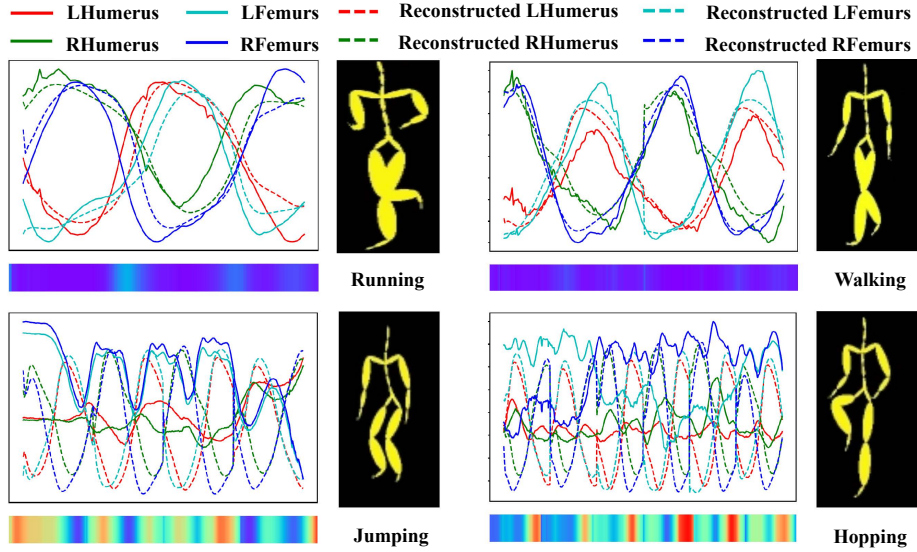


Figure 2: Reconstruction results of motion time series.

Fig 4.3 shows the reconstruction results of walking, running, jumping, hopping with corresponding conditional data, and their corresponding heatmap. In the running and walking series, the dashed line (reconstructed data) matches well with the solid line (origin data) while reconstructions of jumping and hopping deviate far from the origin data. The results show the ability of MissGAN to reconstruct different categories of time series given corresponding conditional dimensions.

Furthermore, to verify the effectiveness of conditional information, we concatenate two sequences. The first one consists of two running cases labeled running and walking respectively. The second one consists of two walking cases with one running case inserted to the middle whose conditional information is labeled as walking. The reconstruction error showed by heatmap (see Fig 4.4) pinpoints both the mislabeled parts are not normal cases, which shows the effectiveness of conditional information. Heatmap points out the degree of deviation from the reconstructed line to the original line in detail, directing people’s attention straight to the error district which reveals the explainability of our results.

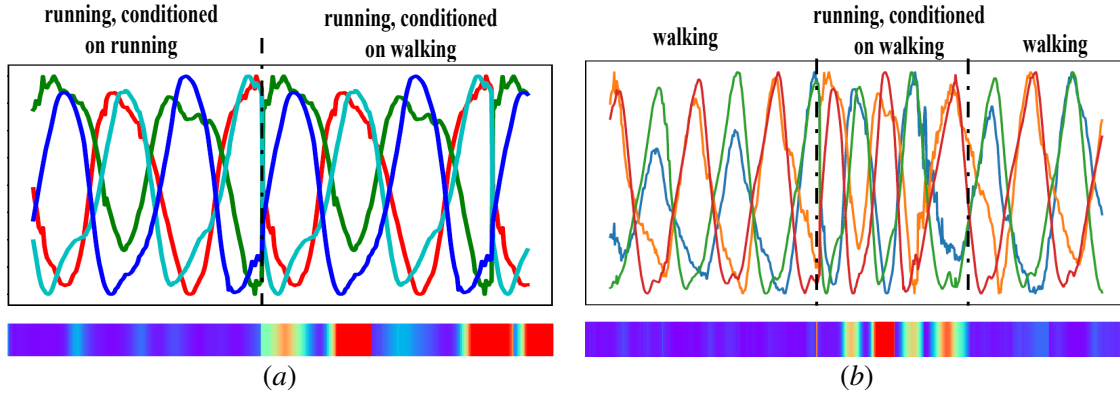


Figure 3: Reconstruction of multi-category series with different conditional dimensions.

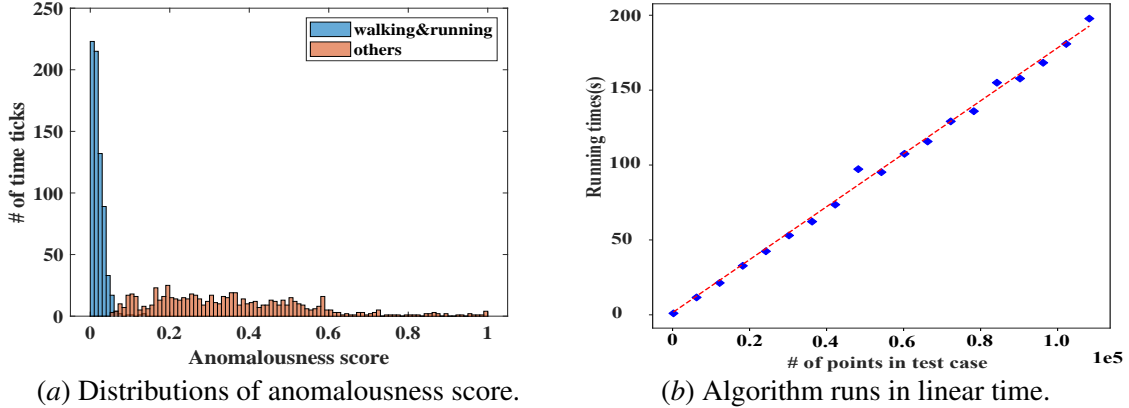


Figure 4: (a). Distributions of anomalousness score between walking&running and others. (b).Results display linear relation of running time and number of points which shows the scalability of MissGAN.

Histogram of anomalousness score is shown in Fig 4(a)subfigure, which reveals the big differences between the distribution of scores of walking&running and others. Scores of walking&running mainly gather below 0.1 while the score of others disperses widely from 0.1 to 1. These results show the great ability of MissGAN in discriminating unusual motions (jumping and hopping) by training with usual motions (walking and running).

#### 4.5. Convergence and Scalability (Q3)

We run our trained model with a test set segmented into different lengths ranging from 240 to 120,000 and record the timespan consumed during running. All the experiments are carried out on a server with a Tesla K80 GPU, implemented in PyTorch. Results showed in Fig 4(b)subfigure display the approximately linear relationship between the number of points and running time which certifies the scalability of our MissGAN.

#### 4.6. Parameter sensitivity (Q4)

To ensure the best performance of our MissGAN, we design architecture experiments concentrating on the regularization parameter  $\lambda$  and dimensions reduced by PCA on SWaT dataset.

We evaluate the effect of regularization by assigning  $\lambda$  the following values: 0.01, 0.1, 1, 10. Fig 5(a)subfigure and Fig 5(b)subfigure depict the result of the regularization parameter experiment. Although the highest ideal F1 score can be obtained at  $\lambda = 0.01$ , its severe fluctuation cannot meet our request. On the contrary, results of  $\lambda = 0.1$  have achieved both a relatively high F1 score and AUC score with a low fluctuation. Hence, we choose 0.1 as our best  $\lambda$ .

Candidates of reduced dimensions range from 2 to 12 with a stride of 2. Detailed results of box plots are shown in Fig 6(a)subfigure and Fig 6(b)subfigure. We can draw a conclusion that the dimension reduced to 6 by PCA has the best AUC score and 8 has the best ideal F1 score. Due to ideal F1 score shall only appear based on well-adjusted parameters and in considering of the generality, we choose dimension reduced to 6 by PCA as our best parameters.

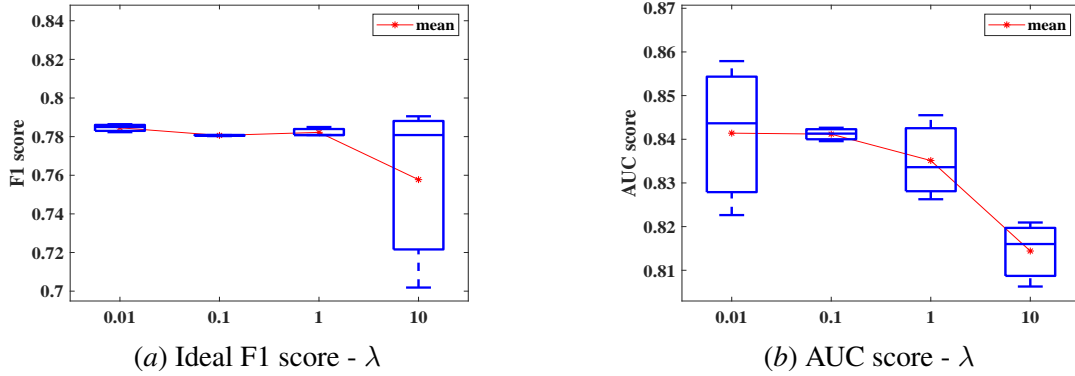


Figure 5: AUC and ideal F1 score of lambda experiments. Numbers on the x-axis stand for the lambda value.

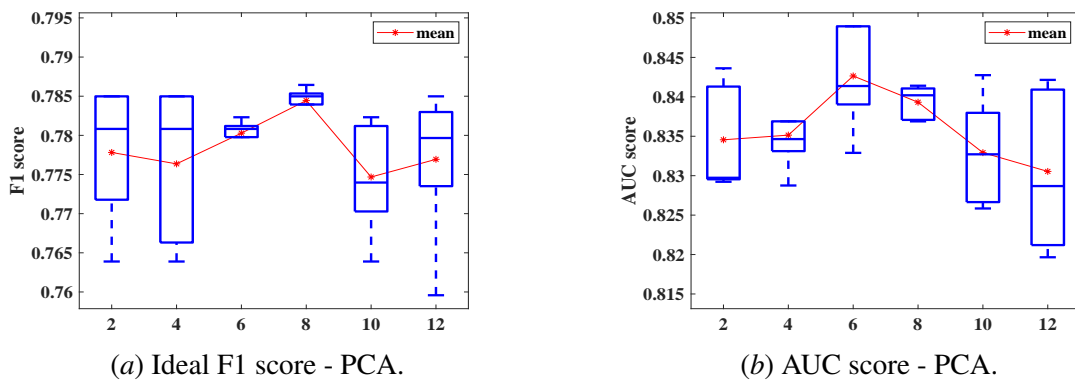


Figure 6: AUC and ideal F1 score of dimension reduction experiments. Model with PCA uses PCA to compress dimensions. Numbers on the x-axis stand for dimensions being reduced to.

## 5. Conclusion

We propose an anomaly detection algorithm for big time series based on reconstruction. Advantages of MissGAN are as follows: 1) Multi-scale reconstruction: MissGAN is trained from coarse to fine-grained segments for best reconstruction performance and MissGAN is able to reconstruct multi-mode time series given different state conditions; 2) Effectiveness: MissGAN outperforms baseline methods on ideal F1 score and AUC score with acceptable fluctuation; 3) Explainability: MissGAN pinpoint ticks of anomalies through displaying anomalousness score shown in Fig 1; 4) Scalability: MissGAN runs linearly in the size of total time series.

To model flexible lengths of time series segments, we reconstruct them using GRU networks. The inherent characteristics of GRU make it model well with smooth time series (i.e., spikes are abnormal). However, this does not limit MissGAN’s applications since normally smooth time series occur in many domains such as infrastructure and traffic monitoring and regularized motion analysis especially for the aged and mobility-impaired people.

## References

- Samet Akcay, Amir Atapour-Abarghouei, and Toby P Breckon. Ganomaly: Semi-supervised anomaly detection via adversarial training. In *Asian Conference on Computer Vision*, pages 622–637. Springer, 2018.
- Fabrizio Angiulli and Clara Pizzuti. Fast outlier detection in high dimensional spaces. In *European Conference on Principles of Data Mining and Knowledge Discovery*, pages 15–27. Springer, 2002.
- Leonard E Baum and Ted Petrie. Statistical inference for probabilistic functions of finite state markov chains. *The annals of mathematical statistics*, 37(6):1554–1563, 1966.
- Raghavendra Chalapathy and Sanjay Chawla. Deep learning for anomaly detection: A survey. *arXiv preprint arXiv:1901.03407*, 2019.
- Varun Chandola, Arindam Banerjee, and Vipin Kumar. Anomaly detection: A survey. *ACM computing surveys (CSUR)*, 41(3):1–58, 2009.
- Pudi Chen, Shenghua Liu, Chuan Shi, Bryan Hooi, Bai Wang, and Xueqi Cheng. Neucast: Seasonal neural forecast of power grid time series. In *IJCAI*, pages 3315–3321, 2018.
- Haeran Cho and Piotr Fryzlewicz. Multiscale and multilevel technique for consistent segmentation of nonstationary time series. *Statistica Sinica*, pages 207–229, 2012.
- Junyoung Chung, Caglar Gulcehre, KyungHyun Cho, and Yoshua Bengio. Empirical evaluation of gated recurrent neural networks on sequence modeling. *arXiv preprint arXiv:1412.3555*, 2014.
- Federico Di Mattia, Paolo Galeone, Michele De Simoni, and Emanuele Ghelfi. A survey on gans for anomaly detection. *arXiv preprint arXiv:1906.11632*, 2019.
- Cristóbal Esteban, Stephanie L Hyland, and Gunnar Rätsch. Real-valued (medical) time series generation with recurrent conditional gans. *arXiv preprint arXiv:1706.02633*, 2017.

- Christos Faloutsos, Valentin Flunkert, Jan Gasthaus, Tim Januschowski, and Yuyang Wang. Forecasting big time series: Theory and practice. In *Proceedings of the 25th ACM SIGKDD International Conference on Knowledge Discovery & Data Mining*, pages 3209–3210. ACM, 2019.
- Ian Goodfellow, Jean Pouget-Abadie, Mehdi Mirza, Bing Xu, David Warde-Farley, Sherjil Ozair, Aaron Courville, and Yoshua Bengio. Generative adversarial nets. In *Advances in neural information processing systems*, pages 2672–2680, 2014.
- Jiawei Han, Jian Pei, and Micheline Kamber. *Data mining: concepts and techniques*. Elsevier, 2011.
- Bryan Hooi, Shenghua Liu, Asim Smailagic, and Christos Faloutsos. Beatlex: Summarizing and forecasting time series with patterns. In *Joint European Conference on Machine Learning and Knowledge Discovery in Databases*, pages 3–19. Springer, 2017.
- Kyle Hundman, Valentino Constantinou, Christopher Laporte, Ian Colwell, and Tom Soderstrom. Detecting spacecraft anomalies using lstms and nonparametric dynamic thresholding. In *Proceedings of the 24th ACM SIGKDD International Conference on Knowledge Discovery & Data Mining*, pages 387–395, 2018.
- Eamonn Keogh, Selina Chu, David Hart, and Michael Pazzani. Segmenting time series: A survey and novel approach. In *Data mining in time series databases*, pages 1–21. World Scientific, 2004.
- Swee Kiat Lim, Yi Loo, Ngoc-Trung Tran, Ngai-Man Cheung, Gemma Roig, and Yuval Elovici. Doping: Generative data augmentation for unsupervised anomaly detection with gan. In *2018 IEEE international conference on data mining (ICDM)*, pages 1122–1127, 2018.
- Tung Kieu, Bin Yang, Chenjuan Guo, and Christian S Jensen. Outlier detection for time series with recurrent autoencoder ensembles. In *28th international joint conference on artificial intelligence*, 2019.
- Aleksandar Lazarevic and Vipin Kumar. Feature bagging for outlier detection. In *Proceedings of the eleventh ACM SIGKDD international conference on Knowledge discovery in data mining*, pages 157–166, 2005.
- Dan Li, Dacheng Chen, Baihong Jin, Lei Shi, Jonathan Goh, and See-Kiong Ng. Mad-gan: Multivariate anomaly detection for time series data with generative adversarial networks. In *International Conference on Artificial Neural Networks*, pages 703–716. Springer, 2019.
- Lei Li, James McCann, Nancy S Pollard, and Christos Faloutsos. Dynammo: Mining and summarization of coevolving sequences with missing values. In *Proceedings of the 15th ACM SIGKDD international conference on Knowledge discovery and data mining*, pages 507–516, 2009.
- Shun Li and Jin Wen. A model-based fault detection and diagnostic methodology based on pca method and wavelet transform. *Energy and Buildings*, 68:63–71, 2014.
- Yonghong Luo, Ying Zhang, Xiangrui Cai, and Xiaojie Yuan. E2gan: end-to-end generative adversarial network for multivariate time series imputation. In *Proceedings of the 28th International Joint Conference on Artificial Intelligence*, pages 3094–3100. AAAI Press, 2019.

- Pankaj Malhotra, Anusha Ramakrishnan, Gaurangi Anand, Lovekesh Vig, Puneet Agarwal, and Gautam Shroff. Lstm-based encoder-decoder for multi-sensor anomaly detection. *arXiv preprint arXiv:1607.00148*, 2016.
- Aditya P Mathur and Nils Ole Tippenhauer. Swat: A water treatment testbed for research and training on ics security. In *2016 International Workshop on Cyber-physical Systems for Smart Water Networks (CySWater)*, pages 31–36. IEEE, 2016.
- Yasuko Matsubara, Yasushi Sakurai, and Christos Faloutsos. Autoplait: Automatic mining of co-evolving time sequences. In *Proceedings of the 2014 ACM SIGMOD international conference on Management of data*, pages 193–204, 2014.
- Antonio Molina and Ferran Pla. Clause detection using hmm. In *Proceedings of the ACL 2001 Workshop on Computational Natural Language Learning (ConLL)*, 2001.
- Thomas Schlegl, Philipp Seeböck, Sebastian M Waldstein, Ursula Schmidt-Erfurth, and Georg Langs. Unsupervised anomaly detection with generative adversarial networks to guide marker discovery. In *International conference on information processing in medical imaging*, pages 146–157. Springer, 2017.
- Neil Shah, Alex Beutel, Brian Gallagher, and Christos Faloutsos. Spotting suspicious link behavior with fbox: An adversarial perspective. In *Data Mining (ICDM), 2014 IEEE International Conference on*, pages 959–964. IEEE, 2014.
- M. Tabb and N. Ahuja. Multiscale image segmentation by integrated edge and region detection. *IEEE Transactions on Image Processing*, 6(5):642–655, 1997.
- Qingfeng Wang, Xuehai Zhou, Chao Wang, Zhiqin Liu, Jun Huang, Ying Zhou, Changlong Li, Hang Zhuang, and Jie-Zhi Cheng. Wgan-based synthetic minority over-sampling technique: Improving semantic fine-grained classification for lung nodules in ct images. *IEEE Access*, 7: 18450–18463, 2019.
- Haowen Xu, Wenxiao Chen, Nengwen Zhao, Zeyan Li, Jiahao Bu, Zhihan Li, Ying Liu, Youjian Zhao, Dan Pei, Yang Feng, et al. Unsupervised anomaly detection via variational auto-encoder for seasonal kpis in web applications. In *Proceedings of the 2018 World Wide Web Conference*, pages 187–196, 2018.
- Chin-Chia Michael Yeh, Yan Zhu, Liudmila Ulanova, Nurjahan Begum, Yifei Ding, Hoang Anh Dau, Diego Furtado Silva, Abdullah Mueen, and Eamonn Keogh. Matrix profile i: all pairs similarity joins for time series: a unifying view that includes motifs, discords and shapelets. In *2016 IEEE 16th international conference on data mining (ICDM)*, pages 1317–1322. Ieee, 2016.
- Houssam Zenati, Chuan Sheng Foo, Bruno Lecouat, Gaurav Manek, and Vijay Ramaseshan Chandrasekhar. Efficient gan-based anomaly detection. *arXiv preprint arXiv:1802.06222*, 2018.
- Leonie Zeune, Guus van Dalum, Leon WMM Terstappen, Stephan A van Gils, and Christoph Brune. Multiscale segmentation via bregman distances and nonlinear spectral analysis. *SIAM journal on imaging sciences*, 10(1):111–146, 2017.

Bin Zhou, Shenghua Liu, Bryan Hooi, Xueqi Cheng, and Jing Ye. Beatgan: anomalous rhythm detection using adversarially generated time series. In *Proceedings of the 28th International Joint Conference on Artificial Intelligence*, pages 4433–4439. AAAI Press, 2019.